Effect of Shunting of Collateral Flow into the Venous System on Arteriogenesis and Angiogenesis in Rabbit Hind Limb

Bao-lin Yang[1,4], Song Wu[2], Xiaoqiong Wu[3], Ming Bo Li[3], Wu Zhu[1], Yinglu Guan[1], Li-Hua Liu[1], Ming-ying Luo[1], Wei-Jun Cai[1], Jutta Schaper[5] and Wolfgang Schaper[5]

[1]Department of Histology & Embryology, School of Basic Medicine, Central South University, Changsha, 410078, Hunan, P.R. China, [2]Department of Orthopedics, The 3rd Xiangya Hospital, Central South University, Changsha, 410078, Hunan, P.R. China, [3]Department of Anatomy & Neurobiology, School of Basic Medicine, Central South University, Changsha, 410078, Hunan, P.R. China, [4]Department of Human Anatomy, School of Basic Medicine, Nanchang University, Nanchang, 330006, Jiangxi, P.R. China and [5]Max-Planck-Institute for Heart and Lung Research, Arteriogenesis Research Group, Bad Nauheim, D-61231, Germany

The aim of this study was to characterize the vascular remodeling in the external iliac artery (EIA) and the lower leg muscles in a rabbit shunt model created between the distal stump of the occluded femoral artery and the accompanying vein. Histology and immunoconfocal microscopy were used in this study. We found that: 1) both endothelial nitric oxide synthase (eNOS) and phosphorylated eNOS (P-eNOS) proteins were significantly increased in the shunt-side EIA; 2) matrix metalloproteinase-2 (MMP-2) expression was 5.5 times in shunt side EIA over that in normal EIA; 3) intercellular adhension molecule-1 (ICAM-1) expression was strongly induced in endothelial cells (EC) and vascular adhension molecule-1 (VCAM-1) expression was significantly increased in both EC and the adventitia of the shunt-side EIA; 4) augmentation of cell proliferation and extracellular proteolysis by macrophage infiltration was observed in shunt-side EIA; 5) cell proliferation was active in shunt side EIA, but quiet in shunt side lower leg's arterial vessels; 6) capillary density in shunt side lower leg muscles was 2 times over that in normal side.

In conclusion, our data demonstrate the paradigm that the power of shear stress takes the reins in arteriogenesis, whereas ischemia in angiogenesis, but not in arteriogenesis.

Key words: arteriogenesis, angiogenesis, macrophages, extracelluar proteolysis, shear stress

I. Introduction

Once chronic occlusion or stenosis is achieved, blood flow is directed toward the region with the lowest resistance via the pre-existent arterioles that now connect a high-pressure with a low-pressure region [22], resulting in increased shear stress. Shear stress, the tractive frictional force exerted by flowing blood on the vascular wall, modulates many physiological [30, 31], biochemical, and molecular [17, 24], responses in *in vitro* and *in vivo* experiments. An increase in shear stress is considered to be responsible for the initiation of arteriogenesis, which is characterized by the growth and remodeling of preexisting arterioles into mature arteries. In addition, several reports have documented that luminal enlargement of the arterial wall is regulated by elevated blood flow, an increase in wall shear stress [2, 15, 28] and tissue ischemia is not required for arteriogenesis [8]. However, it is still difficult to prove or disprove whether ischemia involves arteriogenesis, particularly in the femoral artery or coronary artery occlusion model where the midsection and receiving section of a

Correspondence to: Wei-Jun Cai, M.D., Ph.D., Department of Histology & Embryology, School of Basic Medicine, Central South University, 172 Tong-Zi-Po Road, Changsha, 410078, P.R. China.
E-mail: wjcai@yahoo.com/caiweijun@csu.edu.cn
Wolfgang Schaper and Jutta Schaper, M.D., Max-Planck-Institute for Heart and Lung Research, Arteriogenesis Research Group, Ph.D. Parkstr. 1 D-61231 Bad Nauheim, Germany.
E-mail: wolfgang.schaper@mpi-bn.mpg.de (Wolfgang Schaper), jutta.schaper@mpi-bn.mpg.de (Jutta Schaper)

preexistent collateral vessel locate in the ischemic region.

Previouly, we developed a new animal model for investgating the effects of elevated shear stress on arteriogenesis in which an arteriovenous shunt was created between the distal stump of occluded femoral artery with the accompanying vein in pigs [7, 20]. In this model, the collateral flow is forced to drain directly into the venous system and almost triples the maximal conductance of the normal vasculature, resulting in markedly increased fluid shear stress (FSS) and collateral vessel growth. In addition, elevated collateral flow also caused a significant enlargement of the external iliac artery, whereas draining of collateral flow into the veinous system led to lower leg ischemia. Therefore this model is well-suited for examining whether ischemia contributes to arteriogenesis.

The present study is designed to characterize the histological and molecular changes in the external iliac artery (EIA) and in the lower legs in an arteriovenous shunt model created by a side-to-side anastomosis between the distal stump of the occluded femoral artery and its accompanying vein in rabbit himd limb. For this purpose, expression of adhension molecules, invasion of macrophages, cell proliferation and extracellular proteolysis were investigated by histology and immunoconfocal microscopy with specific antibodies against intercellular adhension molecule-1 (ICAM-1), vascular adhension molecule-1 (VCAM-1), macrophage marker (RAM 11), cell proliferation marker (Ki67), matrix metalloproteinase-2 (MMP-2) and endothelial nitric oxide synthase (eNOS). Our data showed that the involvement of inflammation, extracellular proteolysis and activation of eNOS in iliac arterial remodeling was evident, and that ischemia induced angiogenesis, the formation of new capillaries by sprouting from pre-existent capillaries.

II.   Materials and Methods

Animal model

The present study was performed with the permission of the State of Hessen, Regierungspraesidium Darmstadt, according to Section 8 of the German Law for the Protection of Animals. All experimental protocols used in this research project complied strictly with the Guide for the Care and Use of Laboratory Amimals published by the US National Institutes of Health (NIH Publication No. 85-23, revised 1996). Six adult New Zealand white rabbits were used in this study. After anesthesia with an i.m. injection of midazolam (1 mg/kg) and xylazine (5 mg/kg), the right femoral artery was ligated with two knots. Following the occlusion, an arteriovenous (AV) shunt was created side-to-side between the distal femoral artery stump and the accompanying femoral vein. The left side was used as control. Thereafter the skin was closed with sterile surgical clips. The animals were allowed to recover completely, and housed with free access to water and food. All animals received antibiotic- (Bencylpenicillin) and analgesic treatment (Buprenorphin). We did not observe any gangrene or gross impairment of hindlimb function after femoral artery occlusion and AV fistula creation.

Tissue sampling

At day 14 post-surgery, the animals were re-anesthetized, the external iliac arteries and musculus gastrocnemius tissues from both experimental and normal sides were removed, and immediately frozen in liquid nitrogen, embedded in tissue processing medium (O.C.T) and stored at −80°C till further use.

Histology

Cryosections 5- to 7-μm thick were prepared with Leica CM3050S cryomicrotome (Germany). For elastic fibers' staining, the sections were fixed in 4% paraformaldehyde for 15 min, then stained for elastic fibers according to Weigert' s protocol, Briefly, after fixation, the sections were immersed in Weigert' hematoxylin solution for 10 min, washed in tap water, followed subsequently by 30 min immersion in Resorcin-fuchsin solution, short in 95% alcohol and tap water, 2 min in van Gieson's solution. Finally the sections were dehydrated, cleared and mounted.

Immunohistochemistry

Cryosections were cut 5-μm thick, fixed in 4% paraformaldehyde, except for MMP-2 staining in which

Table 1.   *Primary antibodies and secondary antibodies used in this studies*

Antigen	Clone	Host	Dilution	Company
eNOS	Clone3	Mouse	1:100	Transduction Lab
P-eNOS		Sheep	1:100	Transduction Lab
MMP-2	A-Gel VC2	Mouse	1:200	Biotrend
RAM11	RAM11	Mouse	1:100	Dako
α-SM actin	1A4 FITC*	Mouse	1:300	Sigma
Ki67	MIB-1	Mouse	1:100	Dako
VCAM-1	Rb1/9	Mouse	1:50	Gift#
ICAM-1	Rb2/3	Mouse	1:50	Gift#
Actin-Phallodin	* FITC labeled			Sigma
BS1	Tritc labeled			Sigma
Anto-mouse IgG		Donkey	1:100	Dianova, Germany

* FITC conjugated; # kind gifts from Dr. M.I. Cybulsky, Department of Laboratory Medicine and Pathobiology, University of Toronto, Canada.

Carnoy fixation was used, and pre-incubated in 0.2% BSA-C (Aurion Co.) and thereafter incubated with the primary antibodies (Table 1). Incubation of second antibodies (Table 1) were followed by Cy2 conjugated Streptavidin. The nuclei were stained with 7-aminoactinomycin D or TOTO3 (Molecular Probes). The sections were cover-slipped and viewed with a Leica confocal microscope (Leica TCS SP). Further documentation and image analysis were carried out using a Silicon Graphics Octane work-station (Silicon Graphics) and three-dimensional multi-channel image processing software (Bitplane).

For double staining eNOS with phosphorylated eNOS (P-eNOS), the first sequence was the same as above, after that, sections were washed and blocked by incubation with avidin/biotin reagent (blocking kit, Vector Laboratories Inc). The rest steps were the same as the first sequence.

Incubation with PBS instead of the first antibody was used as negative control to exclude nonspecific binding of the secondary detection system.

Quantitative measurements

The quantification of immunofluorescence intensity of ICAM-1, VCAM-1, eNOS, P-eNOS and MMP-2 was performed with a Leica TCS SP confocal microscope, using the quantitation software of Leica. One channel with format 512 and appropriate filters was used. A full range of gray values from black to peak white (0-pixel to 255-pixel intensity level) was set during the whole process of measurements., The intensity of fluorescence was expressed as arbitrary units $AU/\mu m^2$.

Quantitation of Ki67 positive cells in EIA and small arterial vessels was performed with the confocal micro-scope. The counting was done at 40×, and the ratio of Ki67 positive nuclei to all nuclei of vascular wall was considered as proliferation index in EIA and small arterial vessels,

the number of Ki67 positive nuclei per mm^2 was used as proliferation ratio in skeletal muscles.

Capillary density measurement was performed with the confocal microscope. Tritc-conjugated lectin labeled vessels with a diameter <8 μm were considered capillaries and counted at 40×. Only sections oriented perpendicular to the capillaries were counted. Capillary density was expressed as number/mm^2.

All data are presented as mean±SEM. The t-test was used to examine the difference between normal vessels and growing vessels.

III. Results

Profile of cell proliferation in normal and shunt side EIA

Ki67 antibody was used as a marker to detect cell proliferation in this study. Our data showed that this monoclonal antibody (mouse anti-human Ki67 antigen) worked well with rabbit vascular tissue demonstrated by overlapped staining of Ki67 with nuclei. The cell pro-liferation in shunt-side EIA was apparent with an index of 15% and could be detected in all layers of the vascular wall, whereas cell proliferation was rarely detected in normal EIA, occasionally Ki67 positive cells were found in endothelial cells (Fig. 1, Table 2).

Incubation with PBS instead of Ki67 antibody or other antibodies showed no immunostaining.

Expression of endothelial nitric oxide synthase (eNOS), phosphorylated endothelial nitric oxide synthase(P-eNOS) and MMP-2 in normal and shunt-side EIA

To examine eNOS expression and its activity, dual immunostaining of eNOS with P-eNOS was performed in this study. We found that both positive eNOS and P-eNOS staining were exclusively localized in endothelial cells. In
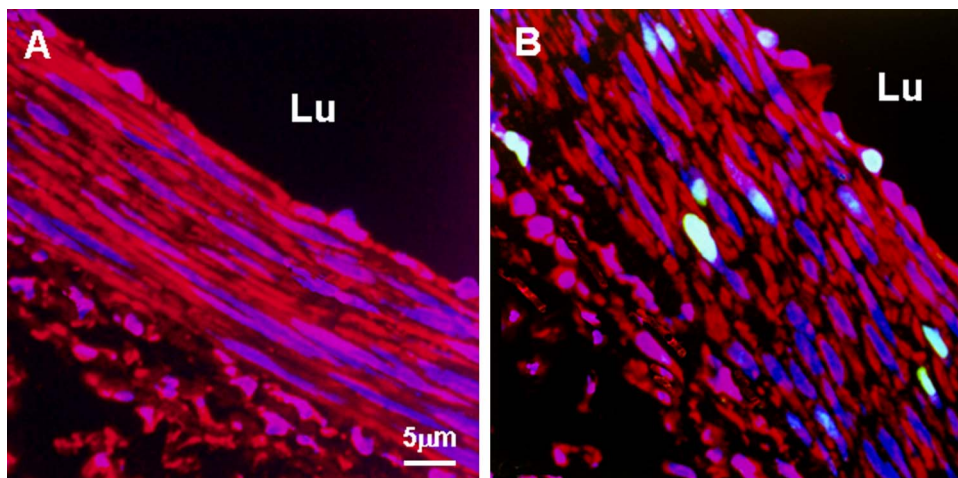

Fig. 1. Representative confocal micrographs of Ki67 immunostaining in normal and shunt side EIA. **A**: normal EIA; **B**: shunt side EIA. Specific fluorescence: green for Ki67, red for Factin; blue for nuclei. Note that in shunt side EIA there were numerous Ki67 positive cells which were distributed in three layers of the wall. Ki67 positive cells were not detected in normal EIA. In addition, the shape of the nuclei was different between normal and shunt side EIAs. Lu: lumen.

Table 2. *Quantitative analysis of immunofluorescence intensity (AU/μm²) of eNOS, P-eNOS, MMP-2, ICAM and VCAM and cell proliferating index (Ki67⁺%) in normal EIA and shunt side EIA, T-test*

Antigen	Normal EIA, n=6	Shunt side EIA, n=6
eNOS	44.51±5.14	108.05±6.30*
P-eNOS	6.15±1.21	25.39±4.35*
MMP-2	20.15±3.26	110.39±8.35*
ICAM	0	70.04±6.08*
VCAM	19.5±2.76	78.78±7.05*
Ki67	0	15.01±4.02*

* $P<0.001$ vs normal EIA.

normal EIA, expression of eNOS was moderate and phosphorylation of eNOS was at a low level (Fig. 2, Table 2). In shunt-side EIA, both amounts of eNOS protein and its activity were significantly increased, they were 2.4 and 3.9 times over that in normal EIA (Fig. 2, Table 2). Expression of MMP-2 in normal EIA was very low in all layers of the wall. It was significantly increased at shunt-side, 5.5 times over that in normal EIA (Fig. 2, Table 2).

Expression of adhensive molecules, ICAM and VCAM and detection of marophages in normal and shunt side EIA

ICAM staining was negative in normal EIA and significantly induced in endothelial cells in shunt-side EIA (Fig. 3, Table 2). In normal EIA, expression of VCAM was low both in endothelial cells and adventitia; but it was 4 times high in shunt-side EIA than that in normal EIA (Fig. 3, Table 2). Macrophage was detected by using RAM11 antibody. In normal EIA, a few macrophages were found in the adventita (Fig. 3). In shunt-side EIA, small amounts of macrophages were detected and invasion of macrophages into the media was also observed (Fig. 3).

Colocalization of macrophages, cell proliferation and extracellular proteolysis in shunt side EIA

The role of macrophages in cell proliferation and extracellular proteolysis in arterial remodeling was examined by immuno-staining of RAM11 and Ki-67 and Weigert's van Gieson staining in serial sections. They were indicative of macrophages, cell proliferation and extracellular proreolysis. There was intensive cell proliferation in the region with an accumulation of macrophages (Fig. 4).
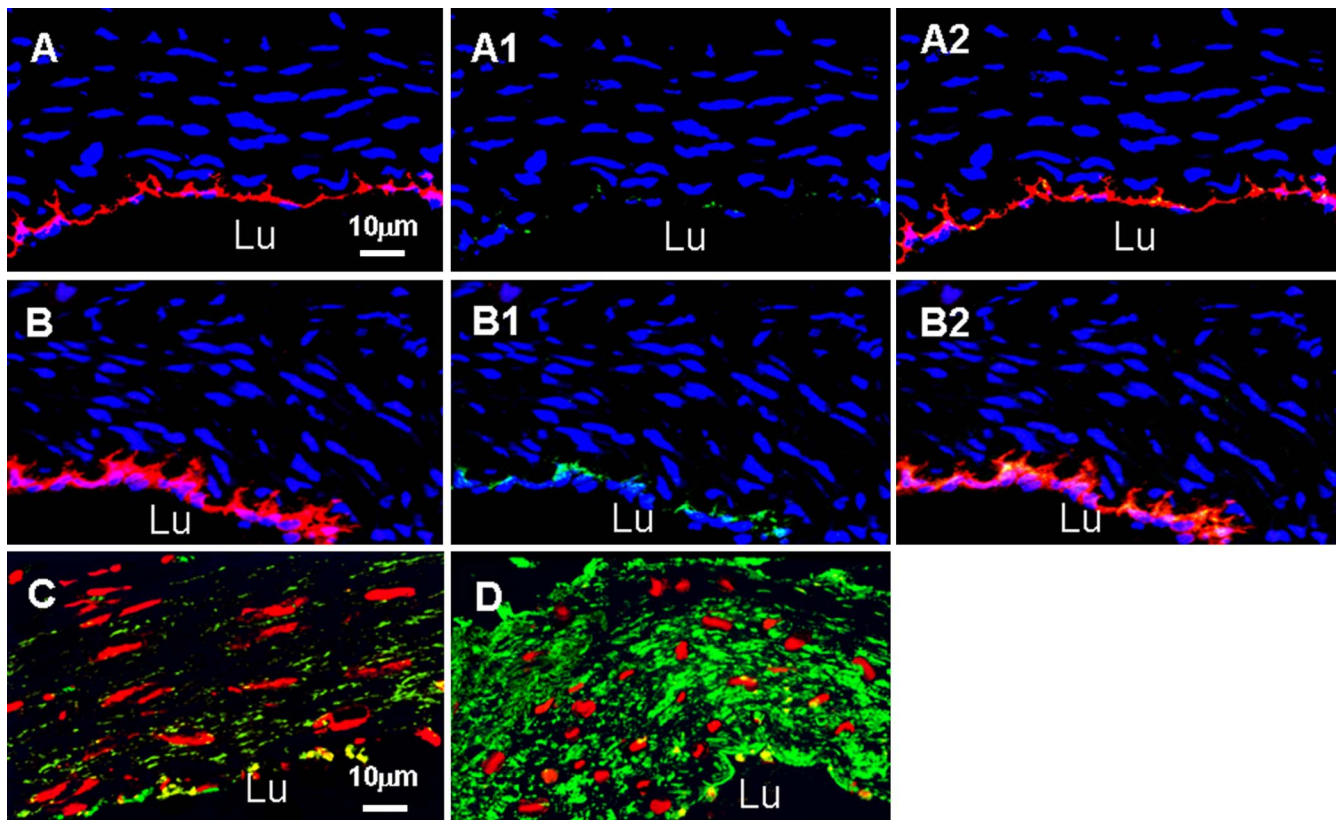

Fig. 2. Confocal micrographs of dual immnostaining of endothelial nitric oxide synthase (eNOS) with phosphorylated eNOS (P-eNOS) and MMP-2 in normal and shunt side EIA. **A** and **C**: normal EIA; **B** and **D**: shunt side EIA. Specific fluorescence: red for eNOS in **A**, **A2**, **B** and **B2**; red for nuclei in **C** and **D**; green for P-eNOS in **A1**, **A2**, **B1** and **B2**; green for MMP-2 in **C** and **D**; blue for nuclei in **A-A2** and **B-B2**. **A2** was merged picture of **A** and **A1**; **B2** was merged picture of **B** and **B1**. Note that strong staining of eNOS, P-eNOS and MMP-2 was present in shunt-side EIA as compared to normal EIA. Lu: lumen.
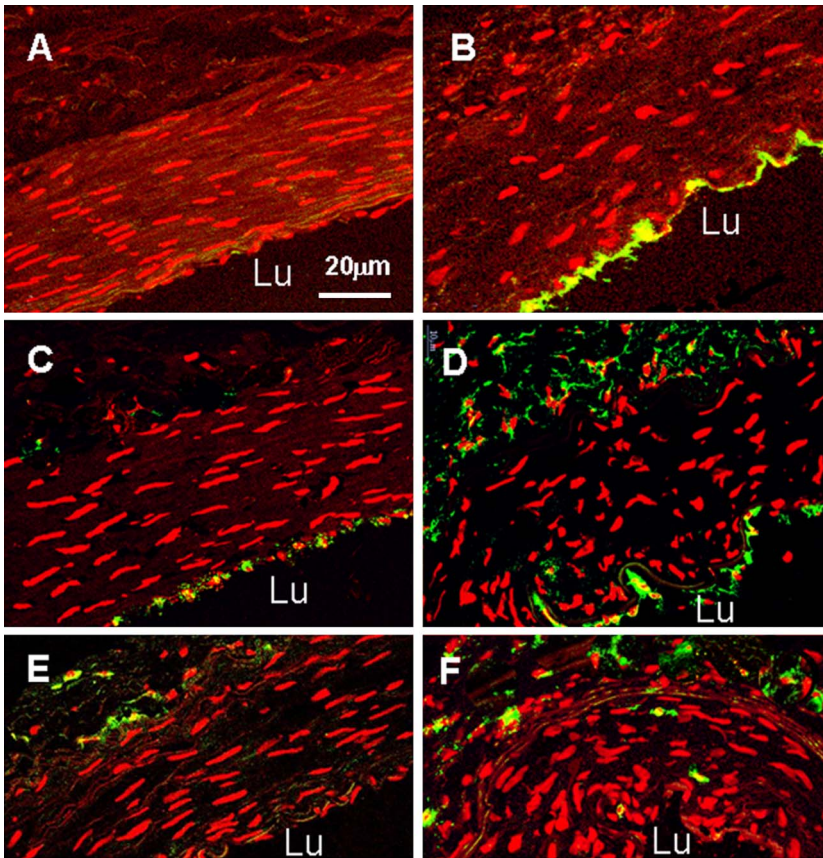
Fig. 3. Confocal micrographs of ICAM, VCAM and RAM11 immunostaining in normal and shunt side EIA. Specific fluorescence: green, red for nuclei. **A**, **C** and **E**: normal EIA; **B**, **D** and **F**: shunt side EIA; **A** and **B**: ICAM. **C** and **D**: VCAM; **E** and **F**: RAM11. Note that in shunt side EIA ICAM was induced in endothelial cells, there was strong staining of VCAM both in the endothelium and adventitia, invasion of macrophages (RAM11) was apparent. Lu: lumen.
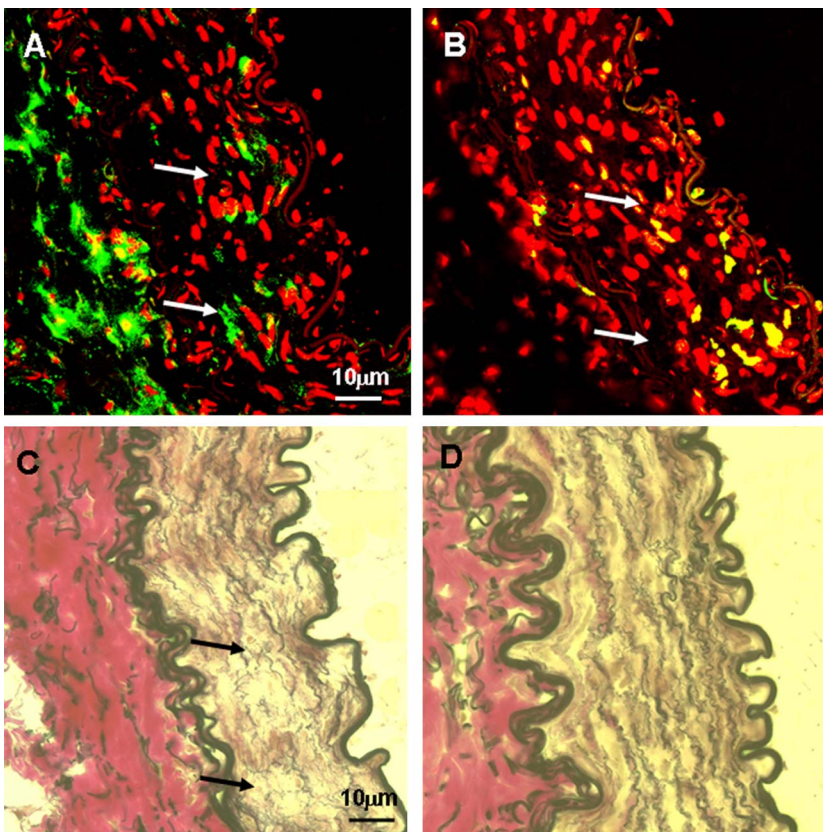

Fig. 4. Micrographs of RAM11 and Ki67 immunostaining and Weigert' van Gieson staining in shunt side EIA (in serial sections). Specific fluorescence: green, red for nuclei. In Weigert' van Gieson staining elastic fiber: black, nuclei: brown, collagen: red, other components: yellow. **A**: RAM11; **B**: Ki67, **C** and **D**: Weigert' van Gieson staining. **A–C**: shunt EIA, **D**: normal EIA. Note that in the region where macrophages (RAM11) were accumulated, there were active high cell proliferation and extracellular proteolysis (indicated by arrows).
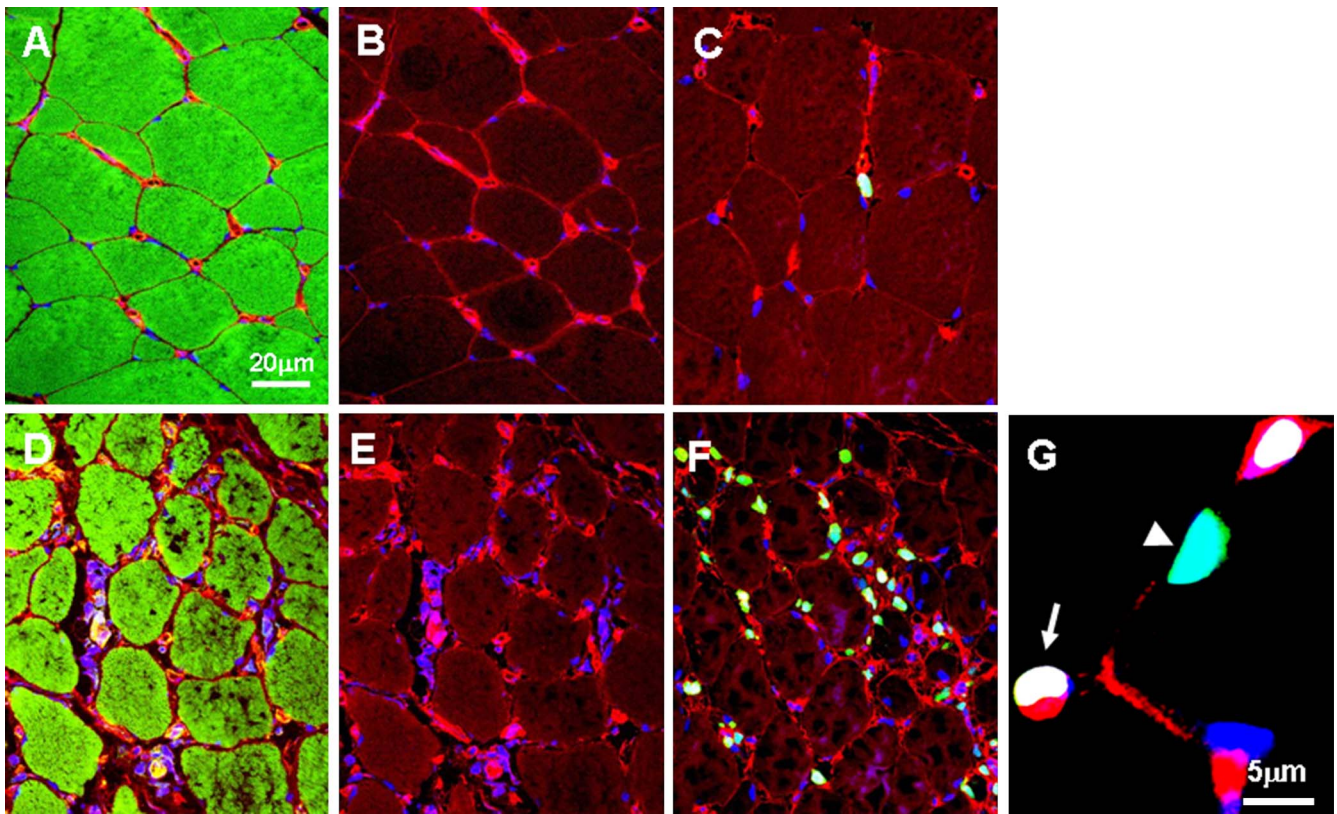
Fig. 5. Confocal micrographs showing angiogenesis in normal and shun side lower leg muscles. **A–C**: normal skeletal muscles, **D–F**: shunt side skeletal muscles. Specific fluorescence: green for F-actin in **A** and **D**, for Ki67 in **C**, **F** and **G**, red for BS1 (marker of endothelial cells), blue for nuclei. Note that cell proliferation and angiogenesis were very active in shunt side skeletal muscles that underwent degeneration. Proliferating cells included endothelial cells (EC) (indicated by arrows) and no ECs indicated by arrowhead.

Capillary density and cell proliferation in normal and shunt-side lower legs

Double staining of F-actin with BS1 was used to mark skeletal muscles and capillaries. In normal *M. gastrocnemius*, the integrity of muscles was evident. In the shunt side, *M. gastrocnemius* showed the signs of degeneration (Fig. 5). The capillary density in normal *M. gastrocnemius* was 780±20/mm². In shunt side it was 1326±40/mm², 1.7 fold than that in normal muscle (Table 3).

In normal *M. gastrocnemius*, cell proliferation was rarely detected, only in non-endothelial cells (Fig. 5,

Table 3. *Quantitative analysis of cell proliferation (Ki67 n/mm²) and capillary density (cap/mm²) in normal and shunt side M. gastrocnemius (n=6) and cell proliferation index (%) in arterial vessels from normal and shunt side M. gastrocnemius (n=6), T-test*

	Normal *M. gastrocnemius*		Shunt *M. gastrocnemius*	
	Skeletal muscle	Arterial vessels	Skeletal muscle	Arterial vessels
Ki67	10±2	0	160±20*	2.01±0.13*
Cap	780±20		1326±40*	

* P<0.001 vs normal EIA.

Table 3); the cell proliferation in shunt-side *M. gastrocnemius* was significantly increased with a 30% index. The proliferating cells included endothelial cells and non-endothelial cells (Fig. 5). In normal lower legs, cell proliferation was not detected in small arteries and arterioles. But it was detected in shunt-side lower legs with a 2% index. However, this cell proliferation was only observed in the endothelial cells, not in the media and adventitia (Fig. 6, Table 3).

The evaluation of the specificity of immunostaining

In this study, pretreatment with 0.2% BSA-C, incubation with PBS instead of the first antibody and contralateral tissue (normal) was used to evaluate the specificity of immunostaining. The results showed these antibodies used in this study were very specific. First, the immunostaining location was specific, for example, Ki67 positive staining was overlapped with nuclear staining, similarly, positive eNOS staining was only present in endothelial cells. Secondly, the staining pattern was supportive, for example, eNOS/ICAM/VCAM was stained negatively or weakly in normal tissue, but strongly in experimental tissue. In addition, incubation with PBS instead of the first antibody showed no immunostaining.
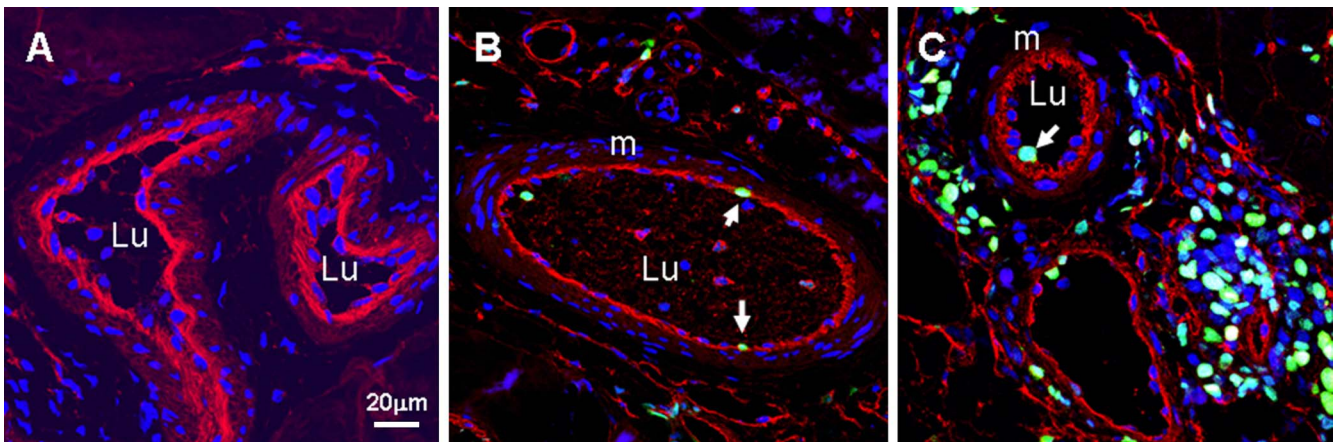
Fig. 6. Confocal micrographs showing arteriogenesis in normal and shun side lower leg muscles. **A**: normal small arteries, **B** and **C**: shunt side small artery and arterioles, respectively. Specific fluorescence: green for Ki67, red for BS1 in **C**, **F** and **G**, red for BS1 (marker of endothelial cells), blue for nuclei. Note that there were Ki67 positive cells in shunt side arterial vessels, but only present in endothelial cells. Lu: lumen, m: media.

IV. Discussion

The results of this study demonstrate that: 1) intensive EIA remodeling was induced by the creation of a side-to-side anastomosis between the distal stump of the occluded femoral artery and its accompanying vein in rabbit hind limb, showing rapid cell proliferation, significant upregulation of eNOS, P-eNOS, MMP-2 and formation of inflammation; 2) in ischemic skeletal muscle tissues, angiogenesis was evident, but not arteriogenesis.

Characteristics of EIA remodeling induced by increased collateral blood flow in rabbit hind limb

We previously reported the expression profiles of eNOS during arteriogenesis in dog heart showing that eNOS expression was increased in growing collateral vessels and returned to normal level in mature vessels. We proposed that increased expression of eNOS was regulated by an increase in fluid shear stress which was generated by a steep pressure gradient along the shortest path within the interconnecting network after arterial occlusion [3]. In the present study, we found that expression of eNOS and its phosphorylation in normal EIA was very low, but both of them were highly upregulated in shunt side EIA. This upregulation of eNOS and its activity could be attributed to increased shear stress since collateral flow in shunt side is two times over the maximal conductance of the normal vasculature [7]. In support of this, previous studies demonstrated that shear stress produced by flowing blood upregulated eNOS expression [32] and that high levels of eNOS mRNA and protein was localized at the areas of higher shear stress *in vivo* [21]. Furthermore, chronic high blood flow by operative arteriovenous fistulas not only led to increased expression of eNOS mRNA and protein, but also increased NOS activity [18].

Arterial enlargement in response to high flow and wall shear stress is endothelial cell dependent. Tohda *et al.* have

shown that deendothelialized segments of flow-loaded rat CCAs fail to dilate [25]. The capacity of the endothelium to sense shear stress is therefore an important determinant of lumen diameter and overall vessel structure remodeling. This capacity is at least partly dependent upon shear stress stimulated eNOS production. Endothelial NO is known as an important systemic vasodilator which can promote EC migration and proliferation. Tronc *et al.* showed that blockade of NO synthesis by NG-nitro-L-arginine-methyl ester (L-NAME) in an arteriovenous fistula model inhibited shear stress mediated vascular remodeling and the underlying mechanism involved NO mediated metalloproteinase activation since L-NAME treatment prevented MMP-2 activation in flow loaded common carotid artery [26, 27]. Most recently, Dai *et al.* reported that endothelial nitric oxide synthase deficiency impairs activation of a cell cycle gene network during arteriogenesis, resulting in collateral vessel rarefaction [5]. Taken together we proposed that increased expression of eNOS and its activity facilitates EIA remodeling.

Proteolysis of elastic materials including the internal and external elastic lamina and elastic fibers in the media and of the basement membranes could be necessary to overcome the structural barriers to arterial remodeling, such as migration and proliferation of endothelial cells and smooth muscle cells and outward expansion. Matrix metalloproteinases (MMPs) play an important role in extracellular matrix digestion. Of the MMPs, MMP-2 can degrade collagen IV, an important component of the basement membrane, as well as collagen V, VII, X, gelatin and elastin. In the present study, we found MMP-2 expressed at low levels in normal EIA, most probably because its SMCs are of the contractile phenotype and quiescent. The turnover of the extracellular matrix proteins was very low. In contrast, in shunt-side EIA, MMP-2 expression was significantly increased and the extracellular proteolysis was very active. In support of this, van-Gieson staining revealed that

there was a distinct elastic network in normal EIA, but became fragmented in shunt side EIA. The finding that there existed an active extracellular proteolysis in shunt side EIA is in agreement with previous reports showing the requirement of extracellular proteolysis for high flow induced arterial enlargement [1, 23]. It should be pointed out that we only detected MMP-2 expression in this study, thus the possibility of the involvement of other proteases in proteolysis could not be ruled out. Further work is needed for clarifying this issue.

The increase in production of adhension molecules, ICAM-1 and VCAM-1 and macrophage invasion by high fluid shear stress was evident in shunt side EIA. This data is in consistence with our previous report showing inflammation was very active in shunt-induced collateral vessels [20]. The relationship between VCAM and ICAM and macrophage in vascular disesase has been well recognized [4]. VCAM-1, which interacts with the monocyte intergrin VLA-4 is specifically upregulated in arterial endothelial cells at lesion-prone areas in hypercholesterolemic mice and rabbits [6, 12]. Moreover, VCAM-1 expression in the luminal endothelium of the grafted veins was found to precede macrophage accumulation in the subendothelium [9]. In addition, a previous report has shown that deficiency or blockade of ICAM-1 inhibited noeintimal thickening of the grafted veins in mice after the vein graft surgery [33]. These findings suggest that adhension molecules, VCAM-1 and ICAM may play a crucial role in macrophage recruitment and subsequent atherosclerosis. The observation that there was a positive correlation between VCAM expression and accumulation of macrophage, and together with the finding that macrophage adhered to endothelial cells and infiltrated into the media in this study are in agreement with the above notion. However, this does not exclude the posibity that other molecules, such as MCP-1, induce macrophage recruitment.

Macrophage could amplify the growth process by secretion of growth factors, such as platelet-derived growth factor (PDGF) and fibroblast growth factors (FGFs) to promote cell proliferation, by production of MMPs to degrade extracellular matrix to faciliate cell migration and outward expansion of the wall. Furthermore, Ito *et al.* showed that local infusion of monocyte chemoattractant protein-1 (MCP-1) markedly increased monocyte adhension and accelerated collateral vessel growth in a rabbit hindlimb ligation model [14]. However, the paradigm showing the close relationshinp among macrophage, cell proliferation and extracellular proteolysis has never been revealed by histology. In this study in serial sections we observed a positive correlation between presence of macrophages, cell proliferation and extracelluar proteolysis. In the region with numerous macrophages, cell proliferation and extracellular proteolysis were very active. This data strengthened the notion that macrophage is an important factor regulating vascular remodeling.

Cell proliferation constitutes an important part of arterial enlargement [23]. In shunt side EIA, a high cell proliferation index was observed. The cell proliferation occurred in all layers of the vascular wall. The greater cell proliferation makes important contributions to rapid growth of EIAs, keeping constant cell density and extracellular matrix production coincident with the increase both in size and in number.

Angiogenesis and arteriogenesis in ischemic lower legs

It was reported in animals with femoral artery ligature and an additional A-V shunt, the peripheral arterial pressure dropped to around 6% of the arterial pressure and only reached around 30% after 4 weeks although collateral blood flow was 2 times over the maximal conductance of the normal vasculature before occlusion since much of collateral blood flow was directly drained into femoral vein [7]. Therefore ischemia was induced in lower leg muscles. We observed that in shunt side m. gastrocnemius was damaged, indicated by F-actin immunostaining. In this muscle, angiogenic reaction was evident, indicated by active cell proliferation, leading to a high capillary density that was 1.7 times over that in normal muscles. The observation that angiogenesis was induced by ischemia in present study is in consistence with a previous report [13].

As mentioned earlier, tissue ischemia is not necessary for arteriogenesis. The notion was further strengthened in the present study by the finding that intensive EIA remodeling was induced by increased blood flow and shear stress. However, it should be noticed that following experimental arterial ligation, angiogenesis occurs coincident with or prior to arteriogenesis [10]. Moreover, angiogenesis occurs in the same vascular bed, distal to the site of arteriogenesis since at least parts of pre-existent collateral arteries locate in the ischemic region [19]. Therefore, it is reasonable to speculate that ischemia may promote arteriogenesis because firstly ischemia may induce an increase in collateral blood flow by increased angiogenesis in the collateral flow-dependent tissue; secondly angiogenesis and arteriogenesis shares some similar molecular mechanisms and physical stimuli, for example, hypoxia-inducible factor-1 induced by ischemia contributes to both processes [11, 16, 19]. However, it is still not known by which mechanism ischemia involves arteriogenesis. In this study limited cell proliferation was observed in endothelial cells in smaller arteries and arterioles of ischemic lower legs, but this mitotic activity was not present in smooth muscle cells which are the most important component of an arterial vessel. Therefore we proposed that ischemia or hypoxia is responsible for angiogenesis, but not for arteriogenesis although it does impact on endothelial cell activation somehow. Our data imply that although there exist some common mechanisms between angiogenesis and arteriogenesis, the most crucial molecules most likely are individual, for example, micro RNA 126 promotes angiogenesis, but has no effect on arteriogenesis [29].

In conclusion, our data demonstrate an intensive external iliac artery remodeling induced by the creation of a side-to-side anastomosis between the distal stump of

the occluded femoral artery and its accompanying vein in rabbit hind limb, characterized by an increased expression of eNOS, MMP-2, ICAM and VCAM and active extracellular proteolysis and mitosis and monocyte invasion. Our data reveal that shear stress takes the reins in arteriogenesis, whereas ischemia dominates in angiogenesis, but not in aretriogenesis. Our data also for the first time provide histology evidence showing macrophage's positive role in cell proliferation and extracellular proteolysis during vascular remodeling.

V.   Acknowledgments

VI.   References

1. Abbruzzese, T. A., Guzman, R. J., Martin, R. L., Yee, C., Zarins, C. K. and Dalman, R. L. (1998) Matrix metalloproteinase inhibition limits arterial enlargements in a rodent arteriovenous fistula model. *Surgery* 124; 328–334; discussion 334–335.

2. Anayiotos, A. S., Jones, S. A., Giddens, D. P., Glagov, S. and Zarins, C. K. (1994) Shear stress at a compliant model of the human carotid bifurcation. *J. Biomech. Eng.* 116; 98–106.

3. Cai, W. J., Kocsis, E., Luo, X., Schaper, W. and Schaper, J. (2004) Expression of endothelial nitric oxide synthase in the vascular wall during arteriogenesis. *Mol. Cell. Biochem.* 264; 193–200.

4. Dansky, H. M., Barlow, C. B., Lominska, C., Sikes, J. L., Kao, C., Weinsaft, J., Cybulsky, M. I. and Smith, J. D. (2001) Adhesion of monocytes to arterial endothelium and initiation of atherosclerosis are critically dependent on vascular cell adhesion molecule-1 gene dosage. *Arterioscler. Thromb. Vasc. Biol.* 21; 1662–1667.

5. Dai, X. and Faber, J. E. (2010) Endothelial nitric oxide synthase deficiency causes collateral vessel rarefaction and impairs activation of a cell cycle gene network during arteriogenesis. *Circ. Res.* 106; 1870–1881.

6. Elices, M. J., Osborn, L., Takada, Y., Crouse, C., Luhowskyj, S., Hemler, M. E. and Lobb, R. R. (1990) VCAM-1 on activated endothelium interacts with the leukocyte integrin VLA-4 at a site distinct from the VLA-4/fibronectin binding site. *Cell* 60; 577–584.

7. Eitenmuller, I., Volger, O., Kluge, A., Troidl, K., Barancik, M., Cai, W. J., Heil, M., Pipp, F., Fischer, S., Horrevoets, A. J., Schmitz-Rixen, T. and Schaper, W. (2006) The range of adaptation by collateral vessels after femoral artery occlusion. *Circ. Res.* 99; 656–662.

8. Fujita, M., Sasayama, S., Ohno, A., Yamanishi, K., Araie, E. and Franklin, D. (1990) Importance of myocardial ischemia for coronary collateral development in conscious dogs. *Int. J. Cardiol.* 27; 179–186.

9. Hanyu, M., Kume, N., Ikeda, T., Minami, M., Kita, T. and Komeda, M. (2001) VCAM-1 expression precedes macrophage infiltration into subendothelium of vein grafts interposed into carotid arteries in hypercholesterolemic rabbits—a potential role in vein graft atherosclerosis. *Atherosclerosis* 158; 313–319.

10. Hershey, J. C., Baskin, E. P., Glass, J. D., Hartman, H. A., Gilberto, D. B., Rogers, I. T. and Cook, J. J. (2001) Revascularization in the rabbit hindlimb: dissociation between capillary sprouting and arteriogenesis. *Cardiovasc. Res.* 49; 618–625.

11. Ho, T. K., Rajkumar, V., Ponticos, M., Leoni, P., Black, D. C., Abraham, D. J. and Baker, D. M. (2006) Increased endogenous angiogenic response and hypoxia-inducible factor-1α in human critical limb ischemia. *J. Vasc. Surg.* 43; 125–133.

12. Iiyama, K., Hajra, L., Iiyama, M., Li, H., DiChiara, M., Medoff, B. D. and Cybulsky, M. I. (1999) Patterns of vascular cell adhesion molecule-1 and intercellular adhesion molecule-1 expression in rabbit and mouse atherosclerotic lesions and at sites predisposed to lesion formation. *Circ. Res.* 85; 199–207.

13. Ito, W. D., Arras, M., Scholz, D., Winkler, B., Htun, P. and Schaper, W. (1997) Angiogenesis but not collateral growth is associated with ischemia after femoral artery occlusion. *Am. J. Physiol.* 273; H1255–H1265.

14. Ito, W. D., Arras, M., Winkler, B., Scholz, D., Schaper, J. and Schaper, W. (1997) Monocyte chemotactic protein-1 increases collateral and peripheral conductance after femoral artery occlusion. *Circ. Res.* 80; 829–837.

15. Kamiya, A. and Togawa, T. (1980) Adaptive regulation of wall shear stress to flow change in the canine carotid artery. *Am. J. Physiol.* 239; H14–H21.

16. Kelly, B. D., Hackett, S. F., Hirota, K., Oshima, Y., Cai, Z., Berg-Dixon, S., Rowan, A., Yan, Z., Campochiaro, P. A. and Semenza, G. L. (2003) Cell type-specific regulation of angiogenic growth factor gene expression and induction of angiogenesis in nonischemic tissue by a constitutively active form of hypoxia-inducible factor 1. *Circ. Res.* 93; 1074–1081.

17. Mitsumata, M., Fishel, R. S., Nerem, R. M., Alexander, R. W. and Berk, B. C. (1993) Fluid shear stress stimulates platelet-derived growth factor expression in endothelial cells. *Am. J. Physiol.* 26; H3–H8.

18. Nadaud, S., Philippe, M., Arnal, J. F., Michel, J. B. and Soubrier, F. (1996) Sustained increase in aortic endothelial nitric oxide synthase expression in vivo in a model of chronic high blood flow. *Circ. Res.* 79; 857–863.

19. Patel, T. H., Kimura, H., Weiss, C. R., Semenza, G. L. and Hofmann, L. V. (2005) Constitutively active HIF-1α improves perfusion and arterial remodeling in an endovascular model of limb ischemia. *Cardiovasc. Res.* 68; 144–154.

20. Pipp, F., Boehm, S., Cai, W. J., Adili, F., Ziegler, B., Karanovic, G., Ritter, R., Balzer, J., Scheler, C., Schaper, W. and Schmitz-Rixen, T. (2004) Elevated fluid shear stress enhances postocclusive collateral artery growth and gene expression in the pig hind limb. *Arterioscler. Thromb. Vasc. Biol.* 24; 1664–1668.

21. Poppa, V., Miyashiro, J. K., Corson, M. A. and Berk, B. C. (1998) Endothelial NO synthase is increased in regenerating endothelium after denuding injury of the rat aorta. *Arterioscler. Thromb. Vasc. Biol.* 18; 1312–1321.

22. Schaper, W. and Pasyk, S. (1976) Influence of collateral flow on the ischemic tolerance of the heart following acute and subacute coronary occlusion. *Circulation* 53(3 Suppl); I57–62.

23. Sho, E., Sho, M., Singh, T. M., Nanjo, H., Komatsu, M., Xu, C., Masuda, H. and Zarins, C. K. (2002) Arterial enlargement in response to high flow requires early expression of matrix metalloproteinases to degrade extracellular matrix. *Exp. Mol. Pathol.* 73; 142–153.

24. Shyy, Y. J., Hsieh, H. J., Usami, S. and Chien, S. (1994) Fluid shear stress induces a biphasic response of human monocyte chemotactic protein 1 gene expression in vascular endothelium. *Proc. Natl. Acad. Sci. U S A* 91; 4678–4682.

25. Tohda, K., Masuda, H., Kawamura, K. and Shozawa, T. (1992) Difference in dilatation between endothelium-preserved and -desquamated segments in the flow-loaded rat common carotid artery. *Arterioscler. Thromb.* 12; 519–528.

26. Tronc, F., Wassef, M., Esposito, B., Henrion, D., Glagov, S. and Tedgui, A. (1996) Role of NO in flow-induced remodeling of the rabbit common carotid artery. *Arterioscler. Thromb. Vasc. Biol.* 16; 1256–1262.

27. Tronc, F., Mallat, Z., Lehoux, S., Wassef, M., Esposito, B. and Tedgui, A. (2000) Role of matrix metalloproteinases in blood flow-induced arterial enlargement: interaction with NO. *Arterioscler. Thromb. Vasc. Biol.* 20; E120–E126.

28. Tulis, D. A., Unthank, J. L. and Prewitt, R. L. (1998) Flow-induced arterial remodeling in rat mesenteric vasculature. *Am. J. Physiol.* 274; H874–H882.

29. van Solingen, C., Seghers, L., Bijkerk, R., Duijs, J. M., Roeten, M. K., van Oeveren-Rietdijk, A. M., Baelde, H. J., Monge, M., Vos, J. B., de Boer, H. C., Quax, P. H., Rabelink, T. J. and van Zonneveld, A. J. (2009) Antagomir-mediated silencing of endothelial cell specific microRNA-126 impairs ischemia-induced angiogenesis. *J. Cell. Mol. Med.* 13; 1577–1585.

30. Walpola, P. L., Gotlieb, A. I. and Langille, B. L. (1993) Monocyte adhesion and changes in endothelial cell number, morphology, and F-actin distribution elicited by low shear stress in vivo. *Am. J. Pathol.* 142; 1392–1400.

31. Wang, D. H. and Prewitt, R. L. (1991) Microvascular development during normal growth and reduced blood flow: introduction of a new model. *Am. J. Physiol.* 260; H1966–H1972.

32. Xiao, Z., Zhang, Z., Ranjan, V. and Diamond, S. L. (1997) Shear stress induction of the endothelial nitric oxide synthase gene is calcium-dependent but not calcium-activated. *J. Cell. Physiol.* 71; 205–211.

33. Zou, Y., Hu, Y., Mayr, M., Dietrich, H., Wick, G. and Xu, Q. (2000) Reduced neointima hyperplasia of vein bypass grafts in intercellular adhesion molecule-1-deficient mice. *Circ. Res.* 86; 434–440.